

Design Development and Characterization of Mannosylated Carbon Nanotubes

¹Jadhav Ketan Namdev, ^{*1}Dr. Sourabh Jain, ²Dr. Gourav Jain, ¹Dr. Karunakar Shukla

¹College of Pharmacy, Dr. A.P.J. Abdul Kalam University, Indore, M.P., India

²Institute of Pharmacy (Diploma), Dr. A.P.J. Abdul Kalam University, Indore, M.P., India

***Email: drsourabhjain@aku.ac.in**

Doi-10.51129/ujpah-june2021-30-1(11)

Abstract - The proposed study was aimed at developing and exploring the efficiency of novel mannosylated MWCNTs. For selective drug delivery to alveolar macrophages, Paclitaxel was selected for incorporation into mannosylated MWCNTs based on its anticancer activity. Hopefully, this delivery system could be safely administered through i.v. route. We expect that this approach will improve management of drug therapy in cancer patients by delivering the drug at controlled rate for prolonged period of time at a desired site. The drug was found to be white to off-white, crystalline powder that was similar in physical appearance as mentioned in I.P. 1996. Melting point of Paclitaxel was near to reported value. Solubility of the drug in different solvents at ambient temperature depicted its solubility in methanol, ethanol, acetone, dimethylsulphoxide and chloroform, while insoluble in distilled and PBS (pH 7.4). Drug entrapment efficiency of Paclitaxel loaded mannosylated MWCNTs was found to be increased.

Keywords: Paclitaxel, Mannosylated MWCNTs, Anticancer, Solubility

Introduction

Cancer that being in the skin or in tissues that line or cover internal organs, there are number of subtype of carcinoma including adenocarcinoma, basal cell carcinoma, squamous cell carcinoma, and transitional cell carcinoma: Cancer that begins in bone cartilage, fat, muscles, or blood vessels, connective tissues or supportive tissues. Cancer that starts blood

forming tissues such as the bone marrow and cause a large number of abnormal blood cells to be produced and entered in the blood. Cancer that begin in the cell of immune system and Cancer that begins in the tissues of brain and spinalcord.

The term lung cancer is used for tumors arising from the respiratory epithelium (bronchi, bronchioles, and alveoli). Mesotheliomas, lymphomas, and stromal tumors (sarcomas) are distinct from epithelial lung cancer. Four major cell types make up 88% of all primary lung neoplasms according to the World Health Organization classification. These are squamous or epidermoid carcinoma, small cell (also called oat cell) carcinoma, adenocarcinoma (including bronchioloalveolar), and large cell carcinoma. The remainder include undifferentiated carcinomas, carcinoids, bronchial gland tumors (including adenoid cystic carcinomas and mucoepidermoid tumors), and rarer tumor types (Minna *et al.*, 2002).

All histologic types of lung cancer are due to smoking. However, lung cancer can also occur in individuals who have never smoked. By far the most common form of lung cancer arising in lifetime nonsmokers, in women, and in young patients (<45 years) is adenocarcinoma. However, in nonsmokers with adenocarcinoma involving the lung, the possibility of other primary sites should be considered. SCLC has scant cytoplasm, small hyperchromatic nuclei with fine chromatin pattern and indistinct nucleoli with diffuse sheets of cells. SCLC comprises about 10%-15% of lung cancers. This type of lung cancer is the most aggressive

strongly related to cigarette smoking with only 1% of these tumors occurring in non-smokers. SCLCs metastasize rapidly to many sites within the body and are most often discovered after they have spread extensively.

NSCLC is the most common lung cancer, accounting for about 85%-90% of all cases. This has three main types designated by the type of cells found in the tumor. It has abundant cytoplasm, pleomorphic nuclei with coarse chromatin pattern, prominent nucleoli, and glandular or squamous architecture. It doesn't grow and spread as fast as small cell lung cancer, and it's treated differently. There are several types of non-small cell lung cancer. (Chu *et al.*, 2006)

Carbon nanotubes (CNTs) have established much recent interest as new entities as a novel drug delivery system for experimental disease diagnosis and treatment because of their unique properties to provide a hollow core appropriate for storing guest molecules (Bianco A; 2004 and Bianco *et al.* 2005). Important properties of CNTs, making them a famous tool more than other nanocarriers, are greater stability, biocompatibility, nonimmunogenicity, ease of size alteration and high drug-loading potential (Martin & Kohli 2003). Internal and external surfaces of CNTs can be modified on an individual basis as required and a variety of functional groups can be generated on their surface in support of further conjugation with targeting ligands as well as drug molecules. The CNTs can be also degraded within human brain tissue by myeloperoxidase (MPO) and hydrogen peroxide (H_2O_2) (Sajid *et al.*, 2016).

Each type of non-small cell lung cancer has different kinds of cancer cells. The cancer cells of each type grow and spread in different ways. The types of non-small cell lung cancer are named for the kinds of cells found in the cancer and how the cells look under a microscope: Carbon nanomaterials, including carbon nanohorns (CNHs), graphenes (GRs), carbon nanorods (CNRs), polyhydroxy fullerenes (PHF) and CNTs, represent safe and efficacious

carrier systems for drug delivery and drug targeting because of their unique physicochemical properties. CNTs were first discovered by Roger Bacon in 1960, and were described fully by Sumio Iijima. CNTs are now the focus of many studies exploring their applications in drug delivery and drug targeting, as well as cosmetic products.

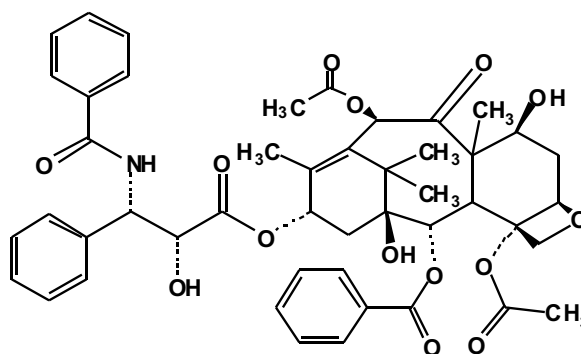
CNTs are ultra-light-weight, tubular, hollow monolithic structures, with a high surface:aspect ratio (length/diameter), rich functional surface chemistry and high drug-loading capacity. They are also biocompatible, nonimmunogenic, and photoluminescent, making them attractive nanocarriers for drug delivery and imaging. CNTs do not require any type of fluorescent labeling for detection because they can be detected directly because of their electron emission properties. CNTs are available as SWCNTs, DWCNTs, TWCNTs and MWCNTs, with cylindrical graphitic layers.

Each type of non-small cell lung cancer has different kinds of cancer cells. The cancer cells of each type grow and spread in different ways. The types of non-small cell lung cancer are named for the kinds of cells found in the cancer and how the cells look under a microscope

Material and Methods

Drug profile

Paclitaxel



Preparation and Characterization:

The present work was aimed to prepare and evaluate mannose conjugated carbon nanotubes for the site-specific delivery of an

anticancer drug i.e. Paclitaxel for effective management of lung cancer.

Purification of pristine MWCNTs

Purification of the MWCNTs was carried out using a modified literature procedure [Liu et al; 1998]. The MWCNTs (300 mg) were added to a mixture of 98% H₂SO₄ and 65% HNO₃ (V:V¼ 3:1, 200 mL) and exposed to sonic irradiation at 0°C for 24 h. The MWCNTs were thoroughly washed with ultrapure water and filtered through a micro-porous filtration membrane (F 0.22 µm). They were redispersed in HNO₃ (2.6 M, 200 mL) and refluxed for 24 h, collected by filtration and washed with ultrapure water to neutrality. The product was then dried under vacuum at 50 °C for 24 h.

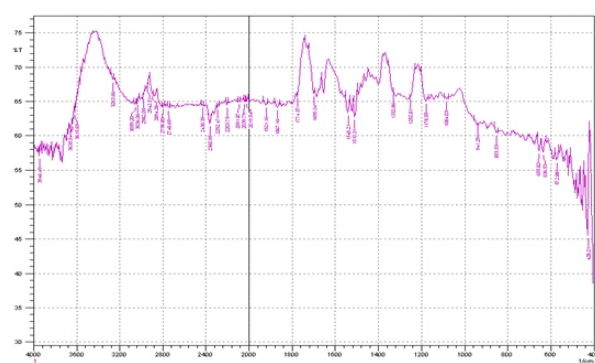


Figure-1 IR of Raw MWCNTs

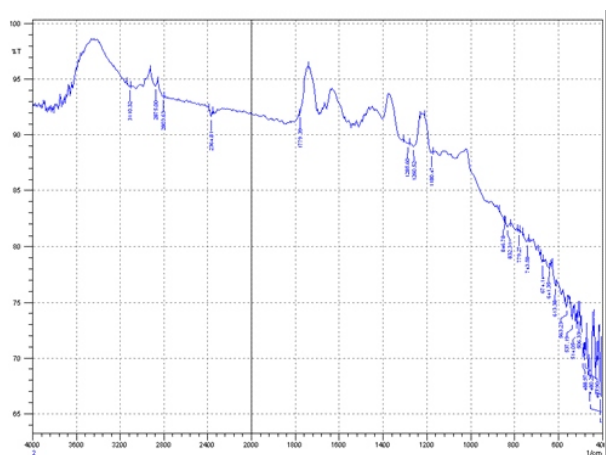


Figure- 2 IR of purified MWCNTs

Preparation of ALG-MWCNTs

MWCNTs (50 mg) were sonicated in sodium ALG solution (100 mg in 0.1 M aqueous NaCl, 100 mL) for 20 min and then stirred at room temperature for 16 h. The modified MWCNTs were collected and washed with ultrapure water by ultracentrifugation to remove unbound ALG, then collected and dried at room temperature to obtain ALG-MWCNTs..

Preparation of CHI/ALG-MWCNTs

The ALG-MWCNTs (40 mg) were sonicated for 20 min and then a CHI solution (6,0 mg in 0.1 M aqueous NaCl and 0.02 M acetic acid, 60 mL) were added. The mixture was stirred for 16 h at room temperature to give the product following ultracentrifugation, washing and drying as described above. (Xiaoke *et al*; 2009)

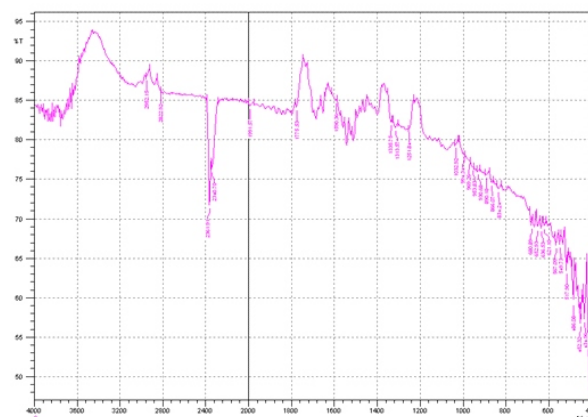


Figure- 3 IR of CHI/ALG-MWCNTs

Preparation of MAN-CHI/ALG-MWCNTs

Mannose (CDH, India) coating was done by ring opening reaction followed by reaction of aldehyde group of mannose with free amine group provided by chitosen on the surface of MWCNTs in sodium acetate buffer (pH 4.0). This led to the formation of Schiff's base (-N=CH-), which may then get reduced to secondary amine (-NHCH-) and remain in equilibrium with Schiff's base. The uncoated mannose and other impurities were removed by dialysis using dialysis membrane (MWCO 1500 Da). The IR spectrum of mannose and mannosylated MWCNTs were taken.

Broad intense O-H stretch and C-O stretch of mannose around 3416.0cm^{-1} and 1094.5cm^{-1} respectively and N-H deformation of secondary amine at 1412.9cm^{-1} confirmed the Schiff base formation and some amine formation via linkage between -CHO of mannose and NH termination of CNTs.

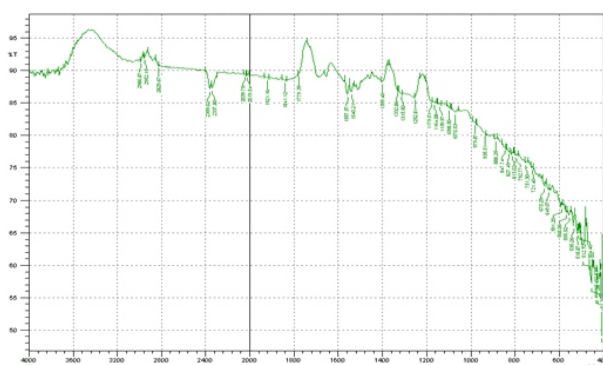


Figure- 4 IR of MAN-CHI/ALG-MWCNTs

D-mannose ($8\ \mu\text{M}$), $28.8\ \text{mg}$ in $20\ \text{ml}$ was dissolved in sodium acetate buffer ($\text{pH}\ 4.0$; $0.1\ \text{M}$) and added to Alginate chitosen modified MWCNTs, followed by heating at $60\pm 0.5^\circ\text{C}$ for an h. The mixture was continuously stirred in a magnetic stirrer (Remi, Mumbai, India) at ambient Temperature for 72 h to ensure the completion of reaction. Mannosylated MWCNTs were purified through a dialysis membrane (MWCO 1214 KDa) against triple distilled deionized water for 12 h to remove unreacted mannose along with other impurities, followed by lyophilization (Hetro Drywinner, Germany).

Paclitaxel loading onto the nanotubes

A solution of $25\ \text{mg}$ ($0.59\ \text{m mol}$) of taxol and $45\ \text{mg}$ ($7.6\ \text{m mol}$) of succinic anhydride in $50\ \text{mL}$ of pyridine was evaporated to dryness in vacuo. The residue was treated with $83\ \text{mL}$ of water, stirred for 20 min, and filtered. The precipitate was dissolved in acetone, water was slowly added, and the fine crystals were collected.

PTX conjugation

PTX was modified by succinicanhydride (CDH) according to the literature, written

above adding a carboxyl acid group on the molecule. MWCNTs ($5\ \text{mg/mL}$,) Functionalization were reacted with $30\ \text{mmol/L}$ of the modified PTX (dissolved in DMSO) in the presence of $5\ \text{mmol/L}$ 1-ethyl-3-(3-dimethylamino propyl) carbodiimidehydrochloride (EDC; Otto) and $5\ \text{mmol/L}$ N-hydroxy sulfo succinimide (Sulfo-NHS, HIMEDIA). The solution was supplemented with PBS at $\text{pH}\ 7.4$. After 6-h reaction, the resulting MWCNT-PTX was purified to remove unconjugated PTX by filtration through 5-kDa MWCO filters and extensive washing.

Characterization of functionalized MWCNTs

Shape and surface morphology

Transmission electron microscope (TEM) photomicrographs were taken at suitable magnification using electron microscopy (TEM) at AIIMS, New Delhi.



Figure- 5 Purified MWCNTs

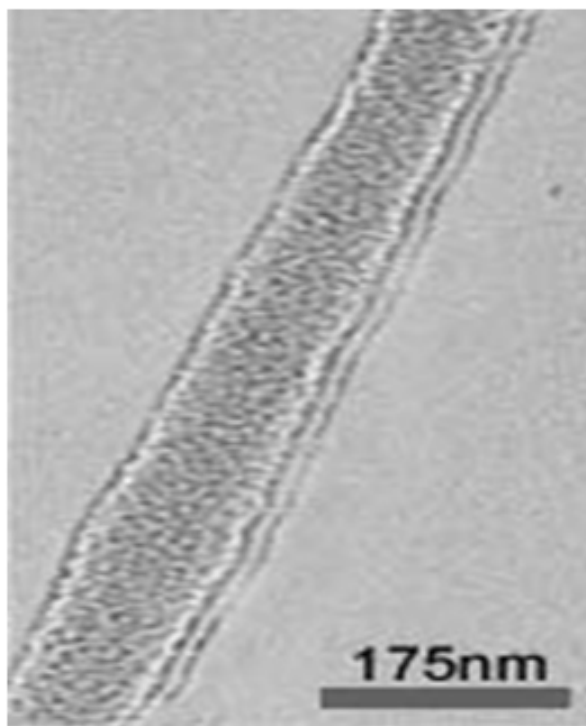


Figure- 6 Alginate Chitosen Coated MWCNTs

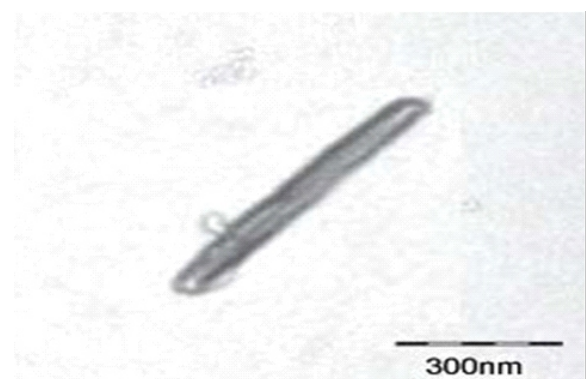


Figure- 7 MAN-CHI/ALG-MWCNTs

The structures of the modified MWCNTs were investigated by TEM. Figure shows the purified nanotubes, after cutting and cleaning, which appear to be smooth and without impurities, indicating that metal particles and amorphous carbon have been completely removed. The cut and purified MWCNTs are generally short (< 500 nm), well separated, and only form small bundles. After coating with ALG and CHI, the polysaccharide chains can be observed on the sidewalls of MWCNTs (Figure-5 and 6). Moreover, the double layered polysaccharide present in CHI/ALG-

MWCNTs is thicker than the purified MWCNTs. The side walls of MWCNTs are poorly defined, presumably due to the thick bilayer of bound CHI/ALG polysaccharides.

Surface charge measurement

The zeta potential of the carbon nanotubes was determined by laser Doppler anemometry using a Malvern Zetasizer also called Doppler Electrophoretic Light Scatter Analyzer. The instrument is a laser-based multiple angle particle electrophoresis analyzer. Using Doppler frequency shifts in the dynamic light scattering from particles, the instrument measures the electrophoretic mobility (or zeta potential) distribution together with the hydrodynamic size of particles (size range 10 to 30 μm) in liquid suspensions by photon correlation spectroscopy measurements.

Estimation of drug entrapment

Drug entrapment of the Paclitaxel in mannosylated MWCNTs was determined by dispersing the known molar concentration of Paclitaxel loaded MWCNTs in PBS: METHANOL in ratio of 60:40. This solution was extensively dialyzed with magnetic stirring (50 rpm; Remi, Mumbai, India) in cellulose dialysis bag (MWCO 1000 Da, Sigma, Germany) against PBS : METHANOL under strict sink condition for 10 min to remove any untrapped drug from the formulation. One mL aliquot was withdrawn and diluted ten times in a volumetric flask with PBS: METHANOL. Absorbance was measured spectrophotometrically (Schimadzu, 1601 Japan) at 274 nm to indirectly estimate the amount of drug entrapped within the system. The dialyzed formulation was then lyophilized and further characterized.

The amount of drug entrapped in Paclitaxel loaded MWCNTs was also determined by employing the similar procedure as reported for Paclitaxel loaded mannosylated MWCNTs. The percentage drug entrapped is recorded in Table-1.

Table-1 Characterization

	Dispersity	Zeta potential mv	% Entrapment efficiency
PTX/MWCNTs	---	-16.03±0.14	76.24±0.23
PTX-MAN- CHI/ALG- MWCNTs	++++	-22.32±1.3	81.23±0.17

In vitro drug release study

The in vitro drug release of paclitaxel from mannosylated CNTs formulation was determined using dialysis tube. The definite amount (5ml) of prepared CNTs formulations, free from any untrapped drug were separately placed into the dialysis tube (MWCO 10 kDa, Hi Media, India), tied at both the ends placed in a beaker containing 50 ml of methanol : phosphate buffer (pH 7.4) 40:60

ratio. The beaker was placed over a magnetic stirrer and the temperature was maintained at 37±1°C throughout the procedure. Samples were withdrawn periodically and after each withdrawal of sample, same volume of PBS was added to the receptor compartment so as to maintain a constant volume throughout the study. The samples were spectrophotometrically (UV-1601 Shimadzu, Japan) analyzed, so as to quantify the Paclitaxel concentration (Table -2 and Figure -8).

Table-2 for % Cumulative drug release

Time (h)	% Cumulative drug release PTX/MWCNTs	% Cumulative drug release PTX/MAN-CHI/ALG-MWCNTs
1	0.90±0.6	1.21±1.5
2	2.41±0.9	3.09±0.7
4	3.98±1.1	4.29±0.8
8	12.39±2.1	13.09±1.7
24	24.83±2.1	28.20±0.8
48	34.8±1.7	37.25±1.11
72	46.05±2.1	50.07±0.7
96	60.65±1.1	69.40±1.9
120	71.3±1.2	81.18±1.8

S.D. ± Mean (n=3)

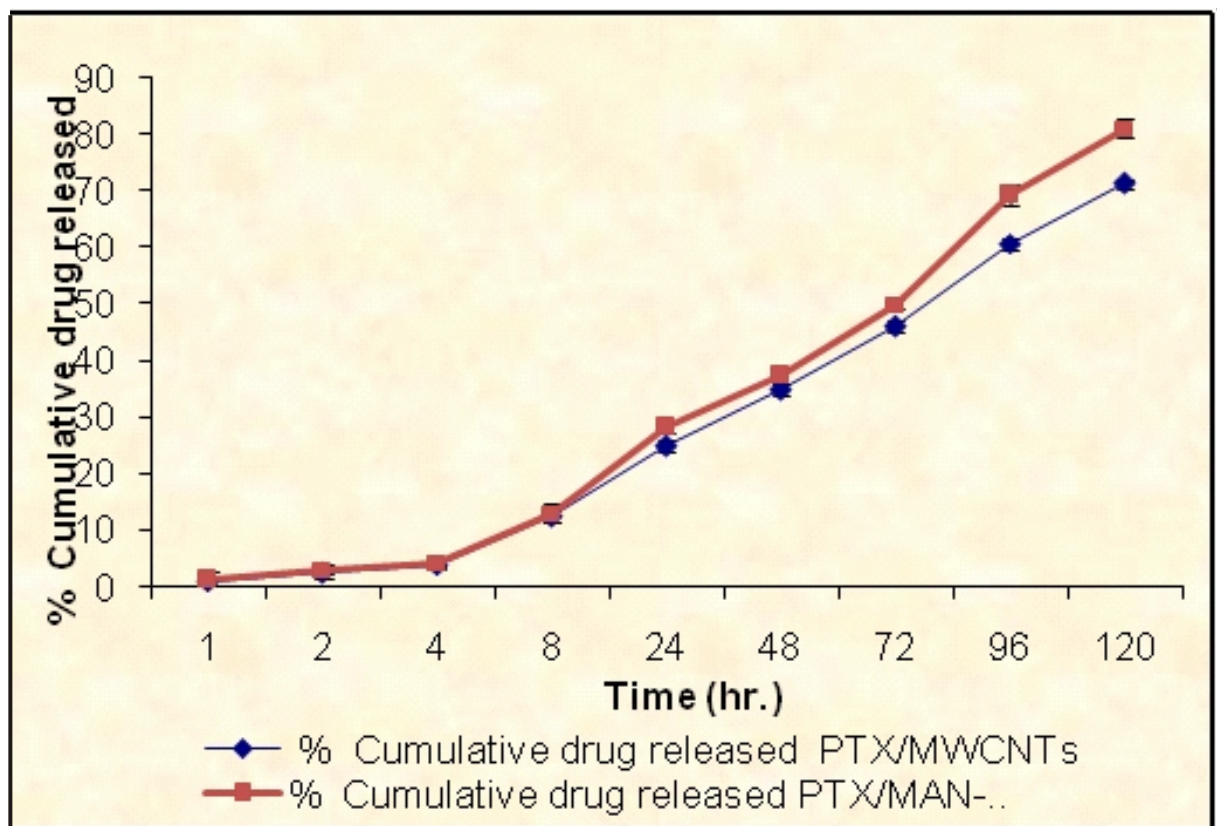


Figure-8 Graph of % Cumulative drug release of PTX/MWCNTs and PTX/MAN-CHI/ALG-MWCNTs

Ex-vivo studies

After preliminary in vitro testing of the formulations for the drug entrapment release rate and stability, the carrier was intended for delivery of drug to animals by parenteral route. However, prior to in vivo studies, the formulations should be evaluated for their efficacy ex-vivo by checking for various interactions. Hence the ex-vivo studies were taken up prior to direct in-vivo efficacy studies in animals.

Cytotoxicity and cell uptake studies

MTT Cytotoxicity assay

Cytotoxicity of paclitaxel loaded MWCNTs and paclitaxel loaded mannosylated carbon nanotubes was determined by measuring the inhibition of cell growth using a tetrazolium dye (MTT) assay. A549 (lung epithelial cancer cell line) was purchased from National Center

for Cell Sciences (NCCS), Pune and cultured in RPMI-1640 medium supplemented with 10% Fetal Calf Serum (FCS) and 2 mM glutamine in a humidified incubator at $37 \pm 1^\circ\text{C}$ and 5% CO_2 atmosphere. A549 cells were seeded at 2×10^5 cells/mL in 96 well plates. The cells were treated with paclitaxel loaded plain MWCNTs and paclitaxel loaded mannosylated MWCNTs. The formulations were added to each well plate with cell line in a decreasing concentration ($10.0 \mu\text{M}$ to $0.01 \mu\text{M}$) simultaneously and incubated for 48 h. Cell viability was analyzed by using the Elisa plate reader at 228 nm. (Yoo et al., 2004)

The drug concentration that reduced the viability of cells was determined by plotting duplicate data points over a concentration range and manually calculating values were obtained using regression analysis.

Table-3 MTTcytotoxicity assay of paclitaxel loaded mannosylated MWCNTs

Paclitaxel Concentration (μ M)	Survival Fraction		
	Free paclitaxel	Paclitaxel loaded plain MWCNTs	Paclitaxel loaded mannosylated MWCNTs
10	45.4	41.3	34.0
20	42.0	39.3	32.9
30	39.8	35.4	30.8
40	36.6	37.5	26.2

S.D.± Mean(n=3)

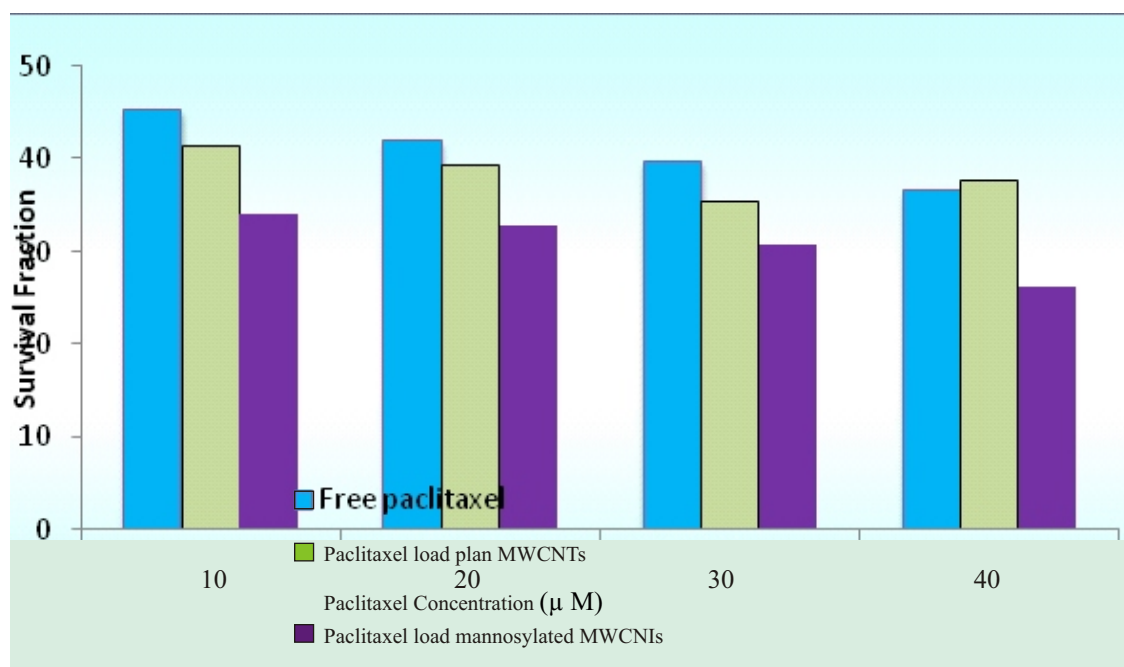


Figure- 9 MTTcytotoxicity assay of PTX loaded mannosylated MWCNTs.

In-vivo studies

The in vivo studies are very important in evaluating the therapeutic efficacy of designed delivery system because in vivo performance is the preliminary step for clinical evaluation of a drug. There are many ways to assess the in vivo performance i.e. measuring the intact drug or metabolite level in the blood or urine, assessing the physiological and biological response in laboratory animals, or by measuring tissue or organ distribution of drug. It is difficult to

predict the behavior of a dosage form on the basis of in vitro studies. Hence in vivo studies in animals or human volunteers are very important before the product is introduced into the market. The significant part of this study was to evaluate in vivo performance of optimized formulations with respect to their capability to deliver the drug precisely to the desired site. The animal studies were conducted with the permission of Institutional Animal Ethical Committee. On the basis of in

vitro evaluation of formulations paclitaxel loaded mannosylated CNTs evaluation.

Standard curve of paclitaxel in blood serum

Blood sample was collected through cardiac puncture in a centrifuge tube which contains heparin (anticoagulant) and centrifuged at 5000 rpm for 10 minutes. Supernatant was collected, then added 2ml of 0.4% ortho phosphoric acid and was deprotenized with equal amount of acetonitrile for half an hour to precipitate proteins. The precipitated proteins were separated by centrifugation at 5000rpm for 10min and supernatant was collected and filtered through 0.45 μ m membrane filter.

Mixture of acetonitrile: methanol: phosphate buffer (38:22:40 v/v/v) was used as the mobile phase. Serum with an appropriate volume of a known amount of drug at a concentration range 1000ng 15000ng/ml of serum and filtered. The filtrate (25 μ l) was injected into a reverse phase C18 150 X 46 mm HPLC column and the eluents were monitored at 228 nm with a flow rate 0.8 ml / min. The peak area of drugs were recorded, the regression of plasma serum concentration of the drug over its peak areas were calculated using the least square method of analysis. The retention time of Paclitaxel was recorded at 7.8 min.

Table-4 Calibration curve of Paclitaxel in blood serum at λ_{max} 228 nm

Concentration (ng/ml)	Peak Area (Observed)	Peak Area (Regressed)	Equation of line:
1000	18380	14216	$y = 20.552x - 4721.4$ $r^2=0.998$
2000	31650	34046	
3000	51659	54776	
4000	73576	77506	
5000	101867	98236	
10000	206233	200886	
15000	300952	305536	

Data 1

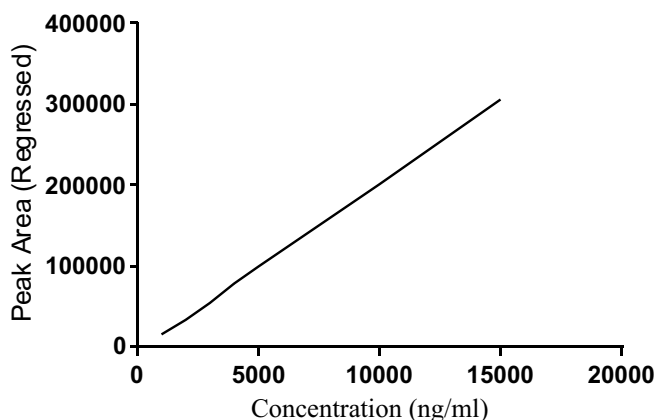


Figure-10 Calibration curve of Paclitaxel in blood serum at λ_{max} 228 nm

Selection of animal

Albino rats of Sprague dawley strain (Hwang et. al., 2008) were chosen for the present study because they offer several advantages as animal model for bio-distribution studies. They are relatively cheap, readily available and easily maintained in laboratory settings. Moreover, their blood volume is large enough to allow frequent blood sampling. This permits Full characterization and determination of the pharmacokinetic profile of the drug.

Biodistribution study in serum and various tissues of rats

The rats were divided into 4 groups, in which first three groups had three animals each and fourth group had only one animal, which served as control. First group was treated with plain paclitaxel solution through i.v. Route. The Paclitaxel loaded plain MWCNTs and Paclitaxel loaded mannosylated MWCNTs dispersion was administered through tail vein in a dose equivalent to Paclitaxel to the animals of second and third group. The animals of fourth group did not receive any drug, which served as control. The blood of animals was

collected from retro orbital plexus of the eye in a centrifuge tube containing heparin sodium (anticoagulant) and centrifuged at 5000 rpm for 10 minutes. Supernatant was collected and acetonitrile was added to precipitate the proteins. The precipitated proteins were settled by centrifugation at 5000 rpm for 10 minutes and supernatant was collected. One ml of collected supernatant was filtered through 0.45 μ M membrane filter and Paclitaxel concentration was determined by HPLC method.

After 1, 8 and 24 hours, the rats were sacrificed and the organs i.e. lungs, liver, and spleen were excised and homogenized in dichloromethane: isooctane mixture. The extracts were separated by centrifugation at 1200 rpm for 10 minutes. The organic extract was dissolved in mobile phase i.e. 0.05 M Water and acetonitrile (60:40). One ml of this was filtered through 0.45- μ m-membrane filter and concentration was determined by HPLC method. The amount of Paclitaxel present in the organs of fourth group animal was determined by simultaneous estimation method using HPLC in Table-5 and Figure-11.

Table-5 Biodistribution of MWCNTs formulations of albino rats.

Time (hrs)	Formulation	Percentage dose recovered		
		Lungs	Liver	Spleen
2	Plain Paclitaxel solution	8.54 \pm 0.69	15.78 \pm 0.96	5.21 \pm 0.24
	Paclitaxel loaded MWCNTs	19.73 \pm 0.94	21.42 \pm 0.84	8.31 \pm 0.32
	Paclitaxel loaded mannosylated MWCNTs	40.53 \pm 0.63	21.39 \pm 0.95	10.15 \pm 1.51
8	Plain Paclitaxel solution	5.31 \pm 0.94	3.61 \pm 0.84	2.85 \pm 0.71
	Paclitaxel loaded MWCNTs	10.63 \pm 1.32	10.95 \pm 0.69	2.49 \pm 0.39
	Paclitaxel loaded mannosylated MWCNTs	20.17 \pm 0.73	24.98 \pm 0.87	1.51 \pm 0.84
24	Plain Paclitaxel solution	1.07 \pm 0.63	2.42 \pm 0.95	1.96 \pm 0.56
	Paclitaxel loaded MWCNTs	2.18 \pm 0.74	3.83 \pm 0.26	2.85 \pm 0.94
	Paclitaxel loaded mannosylated MWCNTs	4.63 \pm 1.32	4.95 \pm 0.69	10.49 \pm 0.39

Mean SD where n= 3

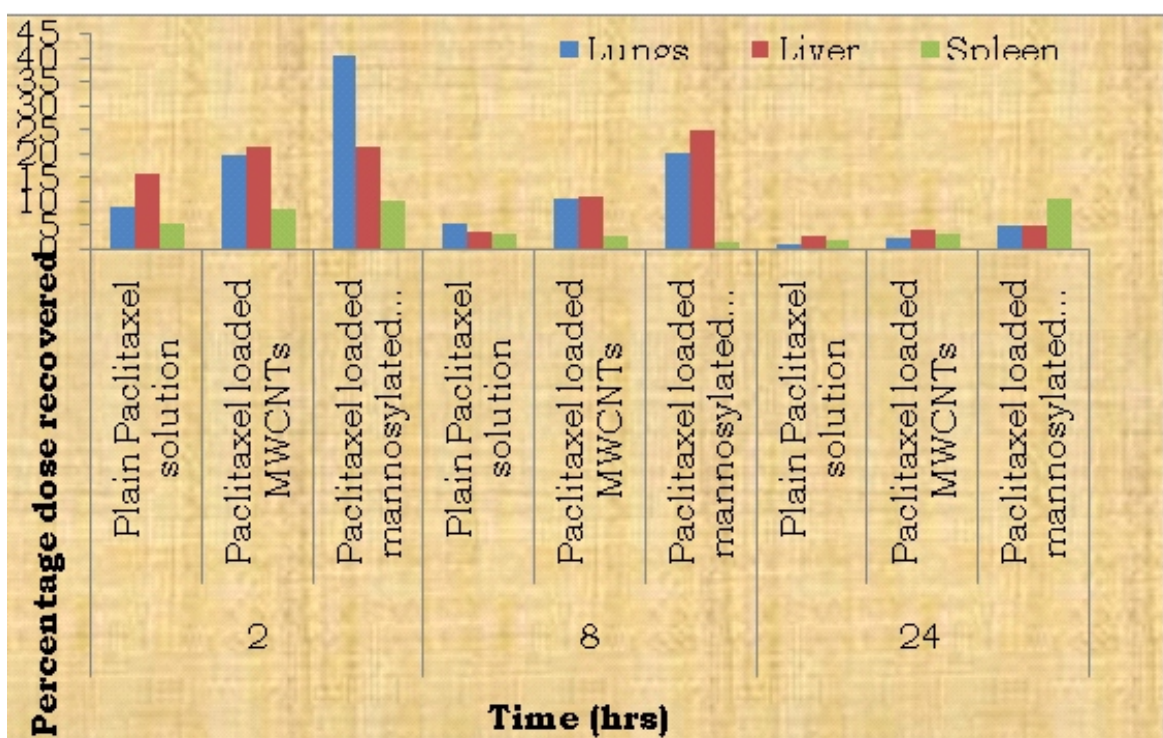


Figure -11 Distribution of paclitaxel in various organs of albino rats after i.v administration of drug

Estimation of paclitaxel in serum

The blood of animals was collected by cardiac puncture in a centrifuge tube containing heparin sodium (anticoagulant) and centrifuged at 5000 rpm for 10 minutes. Supernatant was collected and acetonitrile was added to precipitate the proteins. The precipitated proteins were settled by

centrifugation at 5000 rpm for 10 minutes and supernatant was collected. One ml of collected supernatant was filtered through 0.45- μ m-membrane filter. Same procedure was followed for unconjugated and conjugated CNTs administered rats and Paclitaxel concentration was determined by HPLC method. The observations are shown in Table-6 and Figure-12.

Table-6 *In vivo* drug plasma concentration time profile of various MWCNTs formulations in albino rats

Time (hrs)	% Dose recovered on administration of		
	Plain PACLITAXEL	PACLITAXEL loaded MWCNTs	PACLITAXEL loaded mannosylated MWCNTs
2	48.17 \pm 1.91	28.16 \pm 0.82	15.06 \pm 0.41
8	2.13 \pm 1.19	6.05 \pm 0.58	13.38 \pm 0.55
24	00	1.30 \pm 0.68	7.77 \pm 0.61

S.D. \pm Mean(n=3)

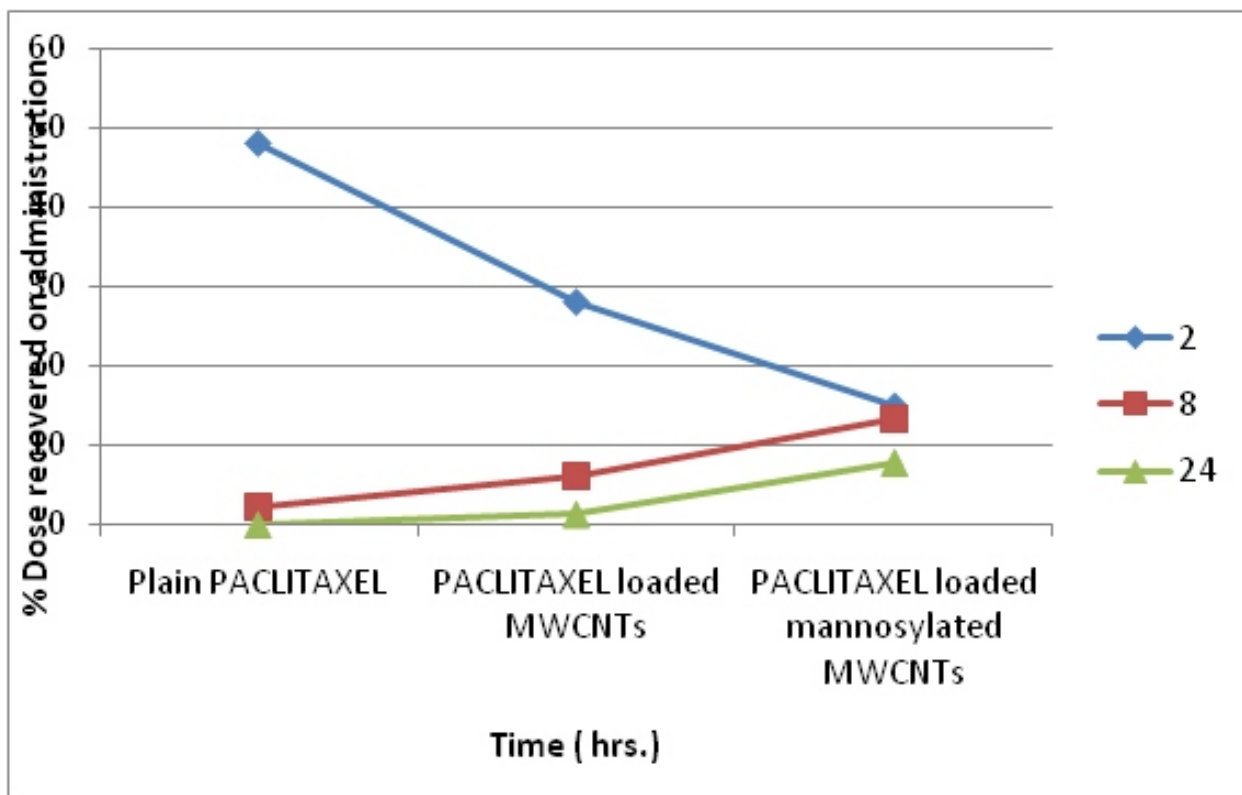


Figure-12 *In-Vivo* drug plasma concentration time profile

Results and Discussion

The purified MWCNTs formulation was optimized to obtain drug entrapment with maximum efficiency. Alginate and chitosen employed in the functionalization of CNTs was first subjected to optimization. The prepared formulation was further characterized on the basis of Shape morphology of the particles which was studied by TEM analysis and zeta potential studies were carried out by using Laser Light Scattering technique (Malvern Instrument).

Drug entrapment was determined by dialysis using a dialysis membrane and was found to be 81.23 ± 0.17 %. Keeping all optimization parameters under consideration, entrapment was found to be optimum in the selected formulation. IR spectroscopy was performed by KBr pellet method to assess the presence of different functional groups over their surface. The pristine MWCNTs showed a peak at 3387

cm^{-1} that can be ascribed to broad OH stretching owing to bound moisture. Peaks at 2955.04, 2893.32, 2337.80 and 1651.12 cm^{-1} suggesting the CNTs backbone and other undefined peaks present in spectrum may be attributed to the presence of amorphous carbon, catalytic and metallic impurities. The IR spectrum of purified MWCNTs exhibits peaks at 2355.4, 1631.9, 1020.6 and 3443.8 cm^{-1} that could be ascribed to the stretching of MWCNTs backbone, C-C stretching, OH in plane bending and broad OH stretching, respectively. Mannosylation was carried out by coupling amine group present on the surface of functionalized CNTs. Broad intense O-H stretch and C-O stretch of mannose around 3410.26 cm^{-1} and 1058.99 cm^{-1} respectively and N-H deformation of secondary amine at 1419.66 cm^{-1} confirmed the schiff's base formation and some amine formation in the linkage between aldehyde of mannose and amine termination groups of MWCNTs.

A comparison was made between drug entrapment, and in-vitro drug release. Particle size of paclitaxel loaded plain CNTs formulation was smaller than paclitaxel loaded mannosylated MWCNTs. This variation may be due to the coating of mannose on the surface of CNTs.

The drug entrapment efficiency of paclitaxel loaded mannosylated CNTs was more as compared to paclitaxel loaded plain CNTs.

In vitro drug release study of both the formulations was carried out using dialysis tube. Formulation PTX / MAN- CHI/ALG-MWCNTs showed a % cumulative drug release of 81.18 ± 1.8 % while PTX /MWCNTs CNTs released up to 71.3 ± 1.2 % upto 120 hours in PBS (pH 7.4). Experiments performed in xenograft models clearly suggest a dose dependent cytotoxicity response i.e. decrease in cell survival fraction with increasing concentration of drug. It was observed that PTX loaded mannosylated MWCNTs exhibited significantly higher cytotoxicity in comparison to PTX loaded plain MWCNTs. Further PTX solution was found to be least cytotoxic. Mannosylated MWCNTs were most cytotoxic and exhibited greater cellular uptake to the greater extent. This may be attributed to ligand-receptor interaction activity which possibly might have promoted their augmented internalization. PTX loaded plain CNTs were slightly less cytotoxic and exhibited less cellular uptake than mannosylated CNTs. A reason may be lack of ligand receptor interaction and the formulation entered the cell only by passive diffusion via EPR effect.

Experiment performed in xenograft model of A549 tumor bearing cells exhibited a linear relationship between fluorescence and drug concentration with about 60% cellular entry of drug (in the formulation) in the concentration range of 100 ng/ml - 300 ng/ml and about 50 % of cellular entry offer the same concentration range of 100 ng/ml-300 ng/ml.

Increased cytotoxicity was observed in case of the mannosylated formulation. It may be due to the fact that the cytotoxicity of CNTs is not dependent on the core, but is most strongly influenced by the nature of CNTs surface. The mannosylated CNTs at a drug concentration of $40 \mu\text{M}$ showed significant cytotoxicity in A549 cell line which may possibly due to attachment of mannose on the surface resulting receptor mediated endocytic uptake.

Bio-distribution studies

In order to determine the fate of paclitaxel loaded mannosylated MWCNTs in vivo, its bio distribution to various organs was investigated. The concentration of paclitaxel in the body depends upon its release, bio distribution, metabolism and excretion from the body. In vivo fates of MWCNTs suggest that uptake of MWCNTs by cancer cells will occur and due to its sustained drug delivery, drug molecule will be available for longer period of time.

In case of free drug maximum dose 48.17 ± 1.91 % was recovered in serum after 2 hour moreover in case of paclitaxel loaded plain MWCNTs and paclitaxel loaded mannosylated CNTs maximum dose recovered in serum was 28.16 ± 0.82 % and 15.06 ± 0.41 % after 2 hour, respectively. These results clearly indicated a drastic reduction in serum concentration of free drug in MWCNTs formulation and may be accounted for the fact that the most of the drug present in blood was entrapped in the MWCNTs.

Maximum amount of drug accumulated in various organs following i.v. administration of free drug viz. $15.780.96$ % in liver (2 hr), 5.21 0.24 % in spleen (2 hr), and 8.54 0.69 % in tumor (2 hr), which were found to be declined constantly.

Encapsulation of drug into MWCNTs was found to be reducing its accumulation in liver, spleen and kidney significantly. Tumor uptake was increased as compared to plain drug solution following the i.v. administration of

paclitaxel loaded MWCNTs. The maximum accumulation in different organs were 21.390.95 % in liver (2hr), 10.15 1.51% in spleen (2hr), and 40.530.63 % in tumor (2 hr). Moreover, the enhance permeability ion and retention effect exerted by MWCNTs promoted their entry to the tumor tissues and reduced access to non tumor tissues.

In case of paclitaxel loaded mannosylated CNTs, uptake of MWCNTs by tumor cells was enhanced due to receptor mediated endocytosis of the CNTs. It was found that after 2 hour, the percent dose recovered from these organs were 21.390.95 % in liver (2hr), 10.15 1.51% in spleen (2 hr), and 40.530.63 % in tumor (2 hr). Besides, the uptake of mannosylated MWCNTs was greater in tumor when compared to plain MWCNTs because of receptor mediated endocytosis. In case of plain CNTs the formulation entered only via passive diffusion.

The above data suggested that although the kidney is a crucial organ for the clearance of bioactives, the mannosylation possibly helped to bypass renal elimination and is finally eliminated after the formulation yielded to metabolism in the liver. The drug levels in liver were increased in case of unconjugated CNTs possibly because of uptake of unconjugated CNTs by mono-nuclear phagocytic system. However the drug level in tumor was also increased in case of uncoated MWCNTs because of indirect action of enhanced residence time of the drug loaded in unconjugated CNTs formulation in the body that promotes distribution of drug to various body organs.

The proposed study was aimed at developing and exploring the efficiency of novel mannosylated MWCNTs. For selective drug delivery to alveolar macrophages paclitaxel was selected for incorporation into mannosylated MWCNTs based on its anticancer activity. Hopefully this delivery system could be safely administered through

i.v. route. We expect that this approach will improve management of drug therapy in cancer patients by delivering the drug at controlled rate for prolonged period of time at a desired site.

The drug was found to be white to off-white, crystalline powder that was similar in physical appearance as mentioned in I.P. 1996. Melting point of Paclitaxel was near to reported value. Solubility of the drug in different solvents at room temperature (25°C) depicted its solubility in methanol, ethanol, acetone, dimethylsulphoxide and chloroform, while insoluble in distilled and PBS (pH 7.4).

The drug was identified for any impurities by chemical tests, UV scanning and IR spectroscopy. The absorption maxima of the drug Paclitaxel in methanol was measured in a Shimadzu (1800, Japan) UV/Visible spectrophotometer and was found to be 228 nm. Infrared spectrum of Paclitaxel confirmed the presence of different functional groups which were identical to the spectra of reference drug given in reference. The standard curves of Paclitaxel were prepared in different media and the absorbance data obtained was subjected to linear regression. The equation of line obtained were $Y = 0.0298X - 0.0009$ and the correlation coefficients were found to be 0.9938 for standard curve of drug in PBS (pH 7.4) which are close to 1.0 indicating good linearity.

Preparation of plain MWCNTs PTX was carried out employing pi pi, interection method which involves the rapid stirring of MWCNTs with paclitaxel solution for 60 minutes . Zeta potential studies were carried out by using Laser Light Scattering technique (Malvern Instrument). Drug loading in the Paclitaxel loaded plain MWCNTs was confirmed by IR spectroscopy as it is showing peaks i.e. C=O stretching at 1073.3cm^{-1} and. Strong N-H bending at 3245.7 cm^{-1} also confirmed the presence of amino group for attaching mannose.

Conclusion

Mannosylation was carried out by coupling amine group present on the surface of CNTs. Broad intense O-H stretch and C-O stretch of mannose around 3509.8 cm^{-1} and 1073.3 cm^{-1} respectively and N-H deformation of secondary amine at 3245.7 cm^{-1} confirmed the schiff's base formation and some amine formation in the linkage between aldehyde of mannose and amine termination groups of MWCNTs. Paclitaxel loaded mannosylated MWCNTs were further subjected to characterization of various parameters i.e. surface morphology, and surface charge. The drug entrapment efficiency of Paclitaxel loaded mannosylated MWCNTs was determined to be $81.23\pm 0.17\%$. Drug entrapment efficiency of Paclitaxel loaded mannosylated MWCNTs was found to be increased.

References

1. Bacon, R. Growth, structure, and properties of graphite whiskers. *Journal of Applied Physics*, 1960, 31(2):283-290.
2. Bianco, A.; Kostarelos, K. and Prato, M. Applications of carbon nanotubes in drug delivery. *Current Opinion in Chemical Biology*, 2005, 9: 674-679.
3. Bianco, A. Carbon nanotubes for delivery of therapeutic molecules. *Expert Opin Drug Deliv.*, 2004, 1(1): 57-65.
4. Chu, E.; DeVita and VT. Jr: Cancer Chemotherapy Drug Manual , 6th ed. Jones & Bartlett, 2006.
5. Liu, J.; Rinzler, A.G.; Dai, H.; Hafner, J.H.; Bradley, R.K.; Boul, P.J. and Smalley, R.E.. *Fullerene pipes. Science*, 1998, 280(5367): 1253-1256.
6. Martin, CR. and Kohli, P. The emerging field of nanotube biotechnology. *Nat Rev Drug Discovery*, 2003, 2:29-37.
7. Minna, J.D., Roth, J.A. and Gazdar, A.F. Focus on lung cancer. *Cancer cell*, 2002, 1(1): 49-52.
8. Sajid, MI.; Jamshaid, U.; Jamshaid, T.; Zafar, N.; Fessi, H. and Elaissari, A. Carbon nanotubes from synthesis to in vivo biomedical applications. *Int J Pharm.*, 2016, 501:278-99.
9. Xiaoke Zhang, Lingjie Meng, Qinghua Lu, Zhaofu Fei, and Paul J. Dyson "Targeted delivery and controlled release of doxorubicin to cancer cells using modified single wall carbon nanotubes" *Biomaterials*, (2009), 6041-6047.